



# Mechanism of the chemical erosion of SiC under hydrogen irradiation

M. Balden<sup>\*</sup>, S. Picarle, J. Roth

*Max-Planck-Institut für Plasmaphysik, EURATOM Association, Boltzmannstr. 2, D-85748 Garching, Germany*

## Abstract

The erosion yield of SiC due to D bombardment has been determined by the weight-loss method as a function of temperature and energy in the range of 20–300 eV up to 1100 K. A temperature dependence exists clearly below 100 eV. For 20 eV D, the yield is 0.5% at 300 K and 1.5% in the maximum at 500 K. Contrary to Si erosion, no formation of silane was observed with mass spectrometry. Hydrocarbons, predominantly CD<sub>4</sub> molecules, are only found at 20 eV. From the erosion of a thin SiC layer investigated using MeV ion beam analysis, segregation and preferential erosion of carbon are ruled out, because the layer thickness decreases while the composition stays constant. As no volatile silane production is detected, it is assumed that sputtering of Si or silane precursors with low binding energy occurs at low ion energies. The mechanism of the chemical erosion of Si in presence of C and absence of C is different. © 2001 Elsevier Science B.V. All rights reserved.

*Keywords:* Chemical erosion; Silicon carbide; Ion irradiation; Ion beam analysis; Plasma facing materials

## 1. Introduction

Plasma facing materials used in future nuclear fusion devices are of high importance since their erosion determines the compound lifetime and eroded particles from the walls contaminate the plasma, dilute or cool it and thus reduce the performance of the device. At present, graphite is the main material used for protection due to its acceptability in existing fusion plasma devices. Beside the favourable thermomechanical properties of carbon-based materials, carbon has the drawback of high chemical reactivity with hydrogen (and oxygen) [1–3].

Great effort is made to replace carbon by other materials. In the current ITER design [3,4] Be is chosen for the main chamber and tungsten for parts of the divertor while C is restricted to surface areas with extreme power load, such as the divertor target plates. High-Z materials (e.g. W, Mo) were already used but

they were detrimental to plasma performance in high confinement phases [5–7]. Often, high-Z wall materials were only tolerable after wall coating with low-Z (C, B, Be) [5,8] or medium-Z (Si) [9,10] layers. The success of siliconisation in ASDEX Upgrade [10] suggests use of SiC as wall material in the main vessel, Si-doped carbon fibre composite material (e.g. NS31 [11]) as divertor target material combined with the conditioning method of siliconisation [9].

In addition, SiC composite materials (SiC<sub>f</sub>/SiC) have been considered as a promising candidate in fusion applications as structural material in advanced scenarios of power plants with a high efficiency factor. The advantages of SiC materials are their excellent capabilities for high-temperature operation, high structural toughness, good thermal-shock resistance, high chemical stability, and low neutron activation [12,13]. Nevertheless, the application of fibre reinforced SiC is limited by their thermal conductivity, thermal stability (>1500 K) and neutron damage behaviour (degradation of mechanical properties) [12,13].

Only a few studies have yet been performed concerning the erosion behaviour by hydrogen bombardment of SiC [14–19]. Some give hints for a possible

<sup>\*</sup> Corresponding author. Tel.: +49-89 3299 1688; fax: +49-89 3299 1212.

*E-mail address:* martin.balden@ipp.mpg.de (M. Balden).

chemical erosion of SiC. It is the aim of the experiments presented in this paper to elucidate the mechanism of the erosion of SiC. Particular interest has been spent on bombardment with low impact energies (20–300 eV) where a temperature-dependent chemical erosion with the formation of volatile molecules has been reported for both constituents, Si and C [2,20–24].

## 2. Experimental

The erosion experiments were performed at the Garching high current ion source [24,25]. Mass-analysed ion beams of  $D_3^+$  were produced with energies above 3 keV and decelerated to the chosen energy by biasing the target without major loss in beam current. Ion fluxes in the order of  $10^{19}$  D/m<sup>2</sup> s were achieved. The ion beam hits the surface perpendicularly. The base pressure was below  $10^{-6}$  Pa rising to about  $10^{-5}$  Pa during bombardment consisting predominantly of the hydrogen isotope used, while the residual gas pressure of water vapour and methane was further reduced using liquid nitrogen cooled shields around the target.

The erosion yield was obtained by measuring the total ion charge and the weight loss with a sensitivity <1  $\mu$ g. The mean mass of eroded particles from SiC was assumed to be 20 amu (mean value of C and Si). This assumption is discussed later. The targets could be heated by electron bombardment from the rear up to 1200 K during ion bombardment. The temperature was monitored by infrared pyrometry calibrated against optical pyrometry to  $\pm 20$  K.

Emitted volatile molecules were monitored during the bombardment using a line-of-sight quadrupole mass analyser [24,25], which is differentially pumped and surrounded by a liquid nitrogen cooled shield to reduce residual gas signals from H<sub>2</sub>O.

Three different kinds of SiC specimens were used as targets: highly polished SiC single crystals, a thin layer of  $\beta$ -SiC (diamond structure) deposited by CVD from SiH<sub>4</sub> and CH<sub>4</sub> on a silicon  $\langle 100 \rangle$  wafer [26,27] and a SiC/SiC composite material (General Atomics [19]). In addition, targets were made from polished pyrolytic graphite cut parallel to the lattice planes (Union Carbide HPG 99) and from Si single-crystal wafers cut perpendicular to the [1 1 1] direction. Prior to the erosion experiments, all samples were annealed in vacuum for 5 min up to at least 900 K.

Ion beam analyses were performed on the layered SiC target after several weight-loss measurements in order to subsequently pursue changes in thickness and composition. A beam of 1.4 MeV protons was collimated to  $1 \times 1$  mm<sup>2</sup> onto the sample. The incident angle was 3° to avoid channelling. Energy distributions of backscattered protons were recorded at a scattering angle of 165°. To obtain simulated spectra and there-

fore, the depth scale for Si and C, the program SIMNRA [28] was used with the cross-section data given therein.

## 3. Results and discussion

### 3.1. Erosion yields of SiC

Fig. 1 shows the temperature dependence of the erosion yields for 20, 100 and 300 eV D impact on different SiC targets. The data for the SiC layer and SiC single crystal agree quite well. Yield data for pure Si and C are included for comparison in Fig. 1 [21,24]. For D impact energies of 100 and 300 eV, the temperature dependence of the sputtering yield is very weak. Nevertheless, the yields for SiC at 20 eV, especially for the SiC layer, clearly show a maximum at about 500 K which confirms the existence of a chemical erosion process. In addition, the yields in the order of  $10^{-2}$  for 20 eV, i.e., below the threshold energy for physical sputtering [25,29] also indicate the presence of this non-collisional erosion process.

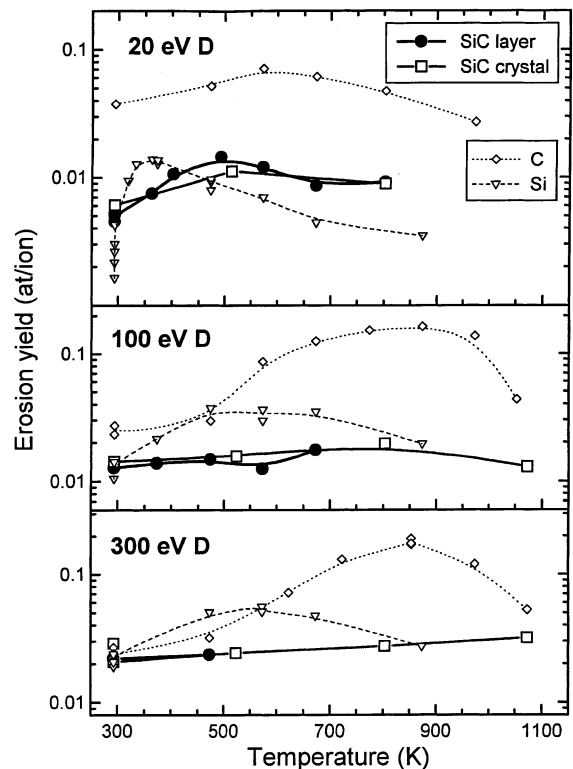


Fig. 1. Temperature dependence of the erosion yields for 20, 100 and 300 eV D impact on the SiC layer on Si (●), SiC single crystal (□ [24]), pure C (◇ [21]) and Si (Δ [24]).

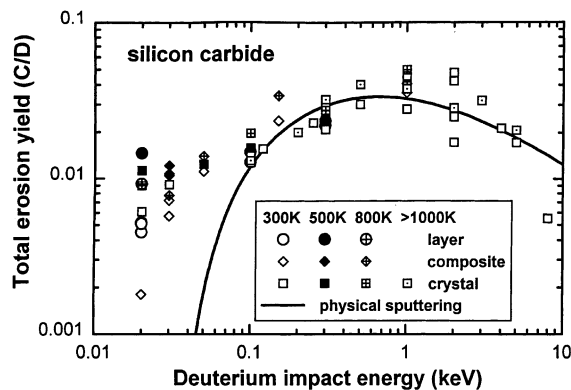


Fig. 2. Energy dependence of the erosion yields for D impact on the SiC layer on Si (circles), SiC single crystal (squares [17,24,25] and new data), and SiC/SiC composite material (diamonds [19] and unpublished data). The target temperature is indicated by empty (300 K), filled (around 500 K), crossed (around 800 K) and dotted symbols (above 1000 K).

A data collection of the energy dependence of the erosion yield for SiC is shown in Fig. 2. For 100 eV and higher impact energies, the yields are well described by the temperature independent physical sputtering [29]. However, even if the yields in previous [17,19,24,25] and present measurements at elevated temperatures around 500–800 K are slightly higher than at 300 K this variation is within the scatter between the different measurement series. Additionally, an indication for chemical erosion products was given earlier (SIMS for 1.5 and 10 keV D impact [14,15]).

Below 100 eV, the experimental erosion yields are higher than those calculated using the physical sputtering principles [29]. The scatter of the data is due to the temperature dependence. Both findings are characteristic of chemical erosion.

### 3.2. Erosion products of SiC

For all investigated D impact energies and target temperatures,  $\text{SiD}_x$  species ( $x = 1, 2, 3, 4$ ) are never observed during the erosion of SiC. However, for 20 eV D impact, clearly a methane signal is observed (Fig. 3(a)) as well as the signal at mass 32, which corresponds to the increased amount of heavier hydrocarbons like  $\text{C}_2\text{D}_4$  at low energies [21]. The highest methane production occurs at about 500 K, which agrees with the results of Plank et al. [19]. At this temperature also the surface Si concentration [19] as well as the yield reach their maximum. For higher energies, the signature of chemically eroded  $\text{CD}_4$  vanishes and no chemically eroded species are detected.

For both constituents of SiC (C, Si) separately, the production of volatile molecules (methane [2,20,21], si-

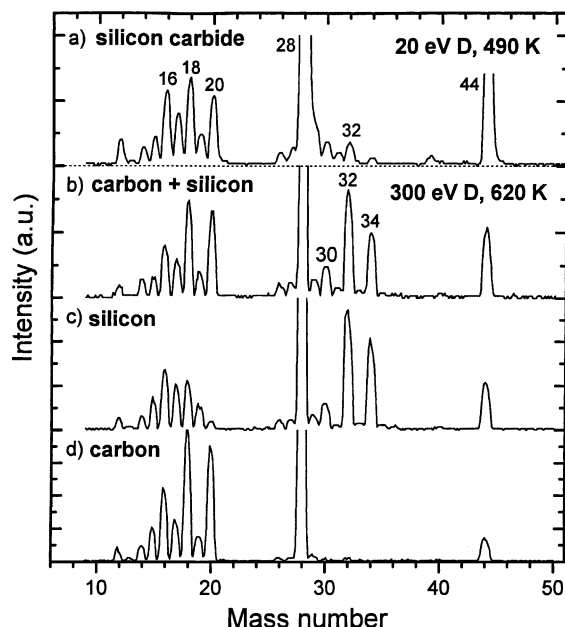


Fig. 3. Mass spectra of the D bombardment on (a) SiC; (b) Si and C simultaneously; (c) Si; (d) C. The D impact energy and target temperature are 20 eV and 420 K for (a) and 300 eV and 620 K for (b)–(d). The bombardment durations before recording the mass spectra (a)–(d) are 5.2, 16, 3 and 0.3 h, respectively.

lane [22–24]) is observed mass spectroscopically. As a difficulty, long transient times were reported for the observation of silane [24]. These transients are visualised in Fig. 4 as the time evaluation of the intensity of the silane signal from the mass spectrometer. During this

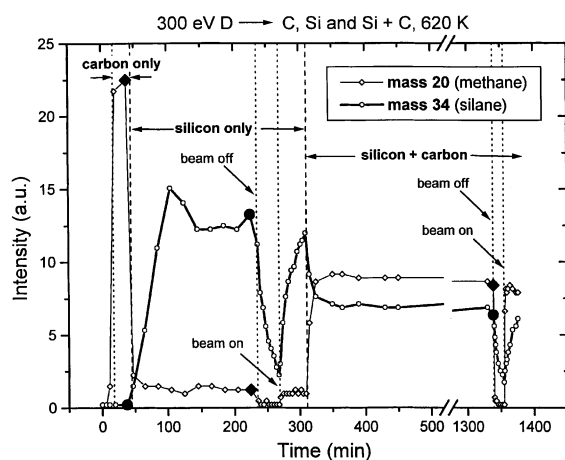


Fig. 4. Time evaluation of the signals of mass 20 and 34 for 300 eV D impact at 620 K. During the experiment, the target is changed (dashed lines) and the D ion beam is switched on and off (dotted lines). The mass spectra corresponding to the large symbols are presented in Figs. 3(b)–(d).

experiment the target was changed from graphite to pure Si and then to half C and half Si by adjusting the D beam on both samples simultaneously. Additionally, the D beam was switched on and off a few times. The transient times for the silane are in the order of 30 min and decrease during the experiment. The methane signal which is also presented in Fig. 4 shows no transient behaviour. Because the transient time of the silane signal decreases and the transient behaviour is also observable after switching off the D beam, it is concluded that this behaviour results from the effect of the chamber walls, especially the liquid nitrogen cooled areas. The walls have to be 'conditioned' before the silane signal reaches steady state.

Figs. 3(b)–(d) show the mass spectra of bombarding Si and C simultaneously, only C, and only Si, respectively. These spectra correspond to the data with the large symbols in Fig. 4. The masses 34, 32 and 30 are prominently observed in Figs. 3(b) and (c). These signals are typical for the cracking products of deuterated silane, i.e.,  $\text{SiD}_3^+$ ,  $\text{SiD}_2^+$  and  $\text{SiD}^+$ . The mass signal at 28 due to CO in the residual atmosphere is dominating in all presented mass spectra of Fig. 3 and the correlated signal of  $\text{CO}_2$  at mass 44 is always observed. In Fig. 3(c) the signals in the range between 12 and 20 are due to the cracking of residual water and methane during bombardment. But the increased peak intensities of 16, 18 and 20 in Figs. 3(a), (b) and (d) are a signature for  $\text{CD}_4$ , which comes from the chemical erosion of carbon.

From bombarding simultaneously the target of pure Si and C, it could be concluded that methane and silane are simultaneously observable, despite the wall 'conditioning' (Fig. 3(b)) and that the transient times are also in the range of 30 min (Fig. 4). Therefore, for all erosion conditions on SiC, the mass signals were followed at least for 4 h. If no chemical bonding (or influence) exists between Si and C, the spectrum for SiC should look like the spectrum from the 'synthetic' Si+C target in Fig. 3(b). It can be concluded that if the Si from SiC is eroded chemically, the mechanism must be different from the chemical erosion of pure Si.

### 3.3. Surface layer composition of SiC

From the observation that the only volatile species released during impact with low energies is methane, it could be argued, that carbon diffuses from the bulk to the surface, where C is then preferentially eroded due to the chemical erosion processes and Si is not eroded. To investigate this possibility, the composition and the thickness of the SiC layer on a Si wafer were determined by ion beam analysis during the erosion. Fig. 5 shows the backscattering spectra of the initial sample, after finishing the series for 20 eV, after several erosion measurements at higher D energies and the corresponding simulated spectra. The decrease of the SiC

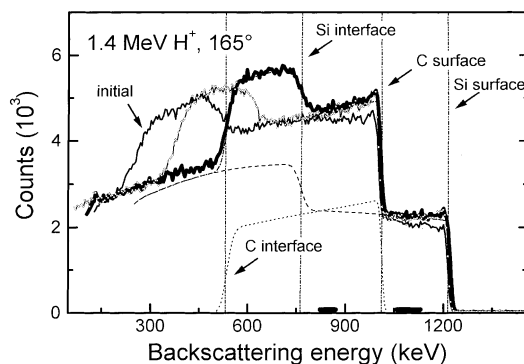


Fig. 5. Backscattering spectra of the SiC layer on Si of the initial sample (thin line), after 20 eV series (thin with circles) and before last weight-loss measurement (thick) (Fig. 6). For the latter spectrum, the corresponding simulated elemental spectra for Si (dashed) and C (dotted) and the positions for Si and C signal from the surface and interface (dash dot dotted) are inserted.

layer thicknesses is visible as a shift of the edges of C and Si at the interface between SiC and Si wafers (shift of the flat top peak). For the three presented spectra, the layer thicknesses are 5.3, 4.8 and 3.9  $\mu\text{m}$ , respectively. Instead of simulating all spectra, an easy way to visualise, that the ratio Si/C did not change from the stoichiometric ratio 1/1 during the erosion, is to plot the ratio of the mean intensity around 850 and 1100 keV, corresponding to the amount of Si and of Si+C (Fig. 6). This ratio is constant during the erosion of the layer. The constancy means that both species are sputtered at the same rate, although in the mass spectra only carbon containing molecules could be found. The calculated change of Si concentration under the assumption, that only C is

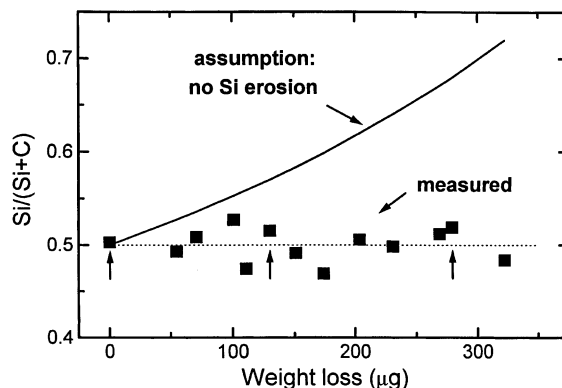


Fig. 6. Si concentration as the scaled ratio of the mean intensities around 850 and 1100 keV (squares) of backscattering spectra versus the accumulated weight loss. Also, the calculated Si concentration changes are shown, if the whole weight loss comes from C erosion. The arrows correspond to the spectra of Fig. 5.

eroded, is also shown. The estimation used for determining the erosion yields, that the mean mass of the eroded particles (Si, C) is 20 amu, and is verified by these results of the backscattering measurements.

#### 4. Summary

The erosion yield of SiC due to D ion bombardment has been determined by the weight-loss method as a function of temperature and energy in the range of 20–300 eV up to 1100 K. The results were compared to those of C and Si. Only in the case of the lowest energy (20 eV), where Si shows a pronounced temperature dependence, a weak temperature dependence exists for SiC with the maximum around 500 K. Chemical erosion clearly exists at low target temperatures and D impact energies below the threshold of physical sputtering. For 20 eV, the chemical erosion yield is 0.5% at 300 K. The experiments were attended by mass spectrometry in the residual gas, showing no formation of silane as chemically eroded compounds, contrary to silicon erosion. Mass-spectrometric measurements show that only at 20 eV the chemically eroded species are hydrocarbons, predominantly CD<sub>4</sub> molecules.

In order to elucidate the erosion mechanism of SiC, the erosion of a thin SiC layer on Si substrate was investigated with ion beam techniques. No change in the layer composition due to the erosion at low ion energies has been observed, while the layer thickness decreases. Therefore, no segregation and no preferential erosion of carbon took place in the erosion of SiC indicating that also Si must be eroded from the SiC surface, and at low D energies (<100 eV) this erosion must be chemically driven.

As no volatile silane production could be detected, it must be assumed that sputtering of Si or silane precursors (or Si<sub>x</sub>C<sub>y</sub>D<sub>z</sub>) with low binding energy occurs at these low ion energies. If the mass spectra of simultaneously bombarded Si and C and the transient times for the observation of silane due to the ‘conditioning’ of the walls are taken into account, the following can be concluded from the absence of silane production: the mechanism of the chemical erosion of Si in presence of C and absence of C is different.

Due to the presence of Si and C atoms next to each other the chemical erosion of both constituents is suppressed for higher D energies (≥100 eV). Because of this

effect, it is tried to reduce the chemical erosion by doping carbon materials [20].

#### References

- [1] R. Parker et al., *J. Nucl. Mater.* 241–243 (1997) 1.
- [2] E. Vietzke, A.A. Haasz, in: W.O. Hofer, J. Roth, (Eds.), *Physical Processes in Plasma–Wall Interaction in Nuclear Fusion*, Academic Press, New York, 1996.
- [3] G. Federici et al., *J. Nucl. Mater.* 266–269 (1999) 14.
- [4] ITER Physics Expert Groups, *Nucl. Fus.* 39 (1999) 2391.
- [5] M.J. May et al., *Plasma Phys. Control Fus.* 41 (1999) 45.
- [6] M. Tokar et al., *Nucl. Fus.* 37 (1997) 1691.
- [7] K. Krieger, H. Maier, R. Neu, ASDEX Upgrade Team, *J. Nucl. Mater.* 266–269 (1999) 207.
- [8] M. Mayer et al., *J. Nucl. Mater.* 241–243 (1997) 469.
- [9] J. Winter et al., *Phys. Rev. Lett.* 71 (1993) 1549.
- [10] V. Rohde et al., in: *Proceedings of the 26th EPS Conference Control Fusion and Plasma Physics*, Maastricht 1999, *Europhysics Conference Abstracts* vol. 23J, 1999, p. 1513.
- [11] C.H. Wu et al., *Fus. Technol. Special Issue* 1996 (1997) 327.
- [12] G.R. Hopkins, in: *Proceedings of the IAEA Symposium on Plasma Physics and Control Nuclear Fusion Research*, Tokyo, Japan, IAEA-CN-33/s3-3, IAEA, Vienna, 1974.
- [13] A. Hasegawa et al., *J. Nucl. Mater.* 283–287 (2000) 128, and references therein.
- [14] M. Mohri et al., *J. Nucl. Mater.* 75 (1978) 7.
- [15] T. Yamashima, in: *Proceedings of the Ninth International Vacuum Congress and Fifth International Conference on Solid Surfaces*, Madrid, Spain, 1983.
- [16] C. Braganza, G.M. McCracken, S.K. Erents, in: *Proceedings of the International Symposium Plasma Wall Interaction*, Jülich, 1976, p. 257.
- [17] J. Bohdansky et al., *J. Nucl. Mater.* 76&77 (1978) 163.
- [18] J. Roth et al., *Radiat. Eff.* 48 (1980) 213.
- [19] H. Plank et al., *Nucl. Instrum. Meth. B* 111 (1996) 63.
- [20] J. Roth, *J. Nucl. Mater.* 266–269 (1999) 51.
- [21] M. Balden, J. Roth, *J. Nucl. Mater.* 280 (2000) 39.
- [22] A.P. Webb, S. Veprek, *Chem. Phys. Lett.* 62 (1979) 173.
- [23] J. Roth, in: R. Behrisch (Ed.), in: *Sputtering at Particle Bombardment II*, Springer, Berlin, 1983.
- [24] M. Balden, J. Roth, *J. Nucl. Mater.* 279 (2000) 351.
- [25] W. Eckstein et al., *Sputtering Data*, Tech. Rep IPP 9/92, Max-Planck-Institut für Plasmaphysik, Garching, 1993.
- [26] R. Siegele et al., *J. Nucl. Mater.* 176&177 (1990) 1010.
- [27] H.P. Liaw, R.F. Davis, *J. Electrochem. Soc.* 132 (1985) 642.
- [28] M. Mayer, *User’s Guide*, Tech. Rep. IPP 9/113, Max-Planck-Institut für Plasmaphysik, Garching, 1997.
- [29] C. García-Rosales et al., *J. Nucl. Mater.* 218 (1994) 8.